

Automated Broadband High-Dynamic-Range Nonlinear Distortion Measurement System

Jonathan R. Wilkerson, *Student Member, IEEE*, Kevin G. Gard, *Member, IEEE*, and Michael B. Steer, *Fellow, IEEE*

Abstract—This paper presents an intermodulation distortion measurement system based on automated feedforward cancellation that achieves 113 dB of broadband spurious-free dynamic range for discrete tone separations down to 100 Hz. For 1-Hz tone separation, the dynamic range is 106 dB, limited by carrier phase noise. A single-tone cancellation formula is developed requiring only the power of the probing signal and the power of the combined probe and cancellation signal so that the phase shift required for cancellation can be predicted. The technique is applied to a two-path feedforward cancellation system in a bridge configuration. The effects of reflected signals and of group delay on system performance is discussed. Spurious frequency content and interchannel coupling are analyzed with respect to system linearity. Feedforward cancellation and consideration of electromagnetic radiation coupling and reverse-wave isolation effects extends the dynamic range of spectrum and vector analyzers by at least 40 dB. Application of the technique to the measurement of correlated and uncorrelated nonlinear distortion of an amplified wideband code-division multiple-access signal is presented.

Index Terms—Broadband, dynamic range, measurement, nonlinear vector signal analyzer, passive intermodulation distortion (PIM).

I. INTRODUCTION

I NTERMODULATION distortion can be the limiting factor in the performance of high-dynamic-range communication systems. Although the active components in the system are designed to meet distortion specifications, often passive components such as transmission lines, filters, combiners, and antennas in the transmit path produce additional distortion after the active components that is difficult to remove. This type of distortion resulting from passive components is known as passive intermodulation distortion (PIM). Two-tone testing is conventionally used to characterize and identify the sources of nonlinear distortion. Characterizing distortion from linear components often requires the measurement of distortion 100 dB or more below the level of applied discrete tones that can be separated by only a few hertz. Measurement when the tones are separated by a few

hertz is required to distinguish the sources of PIM, e.g., electrothermal PIM, nonlinear junction effects, and tunneling [1], [2].

In a nonlinear distortion measurement system, large stimulus tones are typically applied to the device-under-test (DUT), and nonlinear distortion components are generated at much lower power levels than that of the original tones. The original stimulus must be removed from the signal measured at the output of the DUT before reaching the receiver, otherwise the DUT's distortion would be masked by distortion generated in the receiver [3]. To reduce both the stimulus signal and large noise levels simultaneously without effecting the distortion products, filtering or active feedforward techniques [4] are needed to suppress the stimulus signal.

High-dynamic-range measurement systems based on filtering typically use diplexers or notch filters to remove distortion components from sources and amplifiers before application to the DUT. A second filtering stage then removes the stimulus signal before final measurement of the output distortion components by a spectrum or vector analyzer [5]. This scheme, implemented in commercial PIM measurement systems, has the highest achievable dynamic range, but it cannot be used with closely spaced excitation tones because of the finite roll-off of the filters.

Several feedforward cancellation systems for cancelling digitally modulated signals have been reported [6]–[8]. These systems need to be mechanically tuned or optimized. This paper presents the design of an automated feedforward measurement system with high dynamic range which is inherently broadband and which allows measurement with closely spaced signals. In a feedforward measurement system, there will be a difference signal which could be used in a traditional iterative loop to cancel the excitation tones. This was tried, but the extent of cancellation is limited as there must always be an error signal which tends to vary randomly in time although at very low levels. In the measurement system presented here, a predictive formula is used to calculate the phase shift required to automatically cancel a signal based only on the power of the applied signal and of the combined feedforward and applied signals.

The system uses digitally controlled vector modulators in a bridge to suppress the original probe stimulus at a chosen reference plane. The effect of active system components on the linearity of the DUT and cancellation system paths are analyzed. System design parameters are presented based on interchannel coupling and reflected signals. When a two-tone measurement scheme is used, the system achieves 113-dB broadband dynamic range at and above 100-Hz tone separation, reducing monotonically to 106 dB at 1-Hz tone separation. Previously, the authors

Manuscript received September 24, 2009; revised January 22, 2010. First published April 08, 2010; current version published May 12, 2010. This work was supported by the U.S. Army Research Office as a Multi-disciplinary University Research Initiative on Standoff Inverse Analysis and Manipulation of Electronic Systems under Grant W911NF-05-1-0337.

The authors are with the Department of Electrical and Computer Engineering, North Carolina State University, Raleigh, NC 27695-7914 USA (e-mail: jrwilker@ncsu.edu).

Color versions of one or more of the figures in this paper are available online at <http://ieeexplore.ieee.org>.

Digital Object Identifier 10.1109/TMTT.2010.2045525

described a high-dynamic-range distortion measurement system with 95-dB dynamic range in windows between spurious tones resulting mainly from switching power supplies [9]. In the previous system, the dynamic range was limited by electromagnetic coupling between cables, by noise incoherence, by spurious tones from switching power supplies of sources, and by spurious tones from ac power supplies. All of these issues have been addressed in the present system.

The theory of feedforward cancellation in a high-dynamic-range measurement system is presented for discrete tones. Pre-distortion of the phase and amplitude of the original signal(s) is presented as an effective method of cancelling nonlinear effects separate from the DUT including spurious frequency content, distortion content, and group delay. The description of the cancellation theory and system implementation is presented in Sections II–IV for a two-tone stimulus signal. An application of the technique for broadband modulated signals is demonstrated in Section V for the characterization of distortion with a WCDMA signal.

II. FEEDFORWARD CANCELLATION THEORY

Feedforward cancellation relies on feeding forward an anti-phase, equal amplitude version of the signal to be cancelled. The feedforward signal and original signal are then summed and destructively interfere at a reference plane. Signals not related to the feedforward signal are unaffected by the destructive interference. This makes feedforward cancellation an attractive technique for measuring weak intermodulation distortion resulting from discrete-tone signals having narrow tone separations. The amplitude of the feedforward signal must be equal to the probe signal, after the DUT, for cancellation to occur at the reference plane. In this section, a method to predict the phase of the feedforward signal necessary to provide cancellation at a reference plane, under the condition of equal amplitude feedforward and probe signals, is discussed. The equality of signal amplitude is guaranteed through self-characterization of feedforward channel transmission loss in the developed system.

The process of cancelling a signal is mathematically a simple one, requiring only the summation of that signal with an equal amplitude anti-phase signal at the same frequency. However, nonidealities such as small imbalances in amplitude, phase, and group delay must be considered [10]–[13]. Amplitude and phase imbalance, α and $\Delta\phi$, respectively, limit the depth of cancellation achievable, while group delay imbalance limits both the depth and bandwidth of cancellation [10]–[14]. Cancellation performance C_p is described by

$$C_p = 10 \log \left(1 + \alpha^2 - 2\alpha \cos \left(2\pi \cdot \Delta\lambda \left(1 - \frac{f}{f_c} \right) + \Delta\phi \right) \right) \quad (1)$$

where $\Delta\lambda$ is the difference in wavelengths between the two paths normalized to the wavelength of the center frequency f_c and f is the frequency of operation. Mismatch of the group delay between feedforward and DUT signal paths affects cancellation

bandwidth due to the deviation of phase shift between the feedforward and signal paths. This occurs when the frequency shifts away from the center frequency of cancellation. The limiting effect of group delay on the cancellation depth results from the degree of delay mismatch. As the difference in delay grows, so does the rate of phase mismatch with increasing separation from the center frequency. Group delay can be matched to a level acceptable for bandwidth requirements according to (1). Under these conditions, the phase shift and amplitude necessary for cancellation must be obtained.

The amplitude of the feedforward signal necessary to cancel a probe signal at a given reference plane is dependent on the DUT channel transmission characteristic and the DUT loss. These terms need not be separated to cancel the post-DUT probe signal and can be determined directly by a spectral power measurement at the reference plane. In the system developed in this paper, the signal amplitude at the output of the DUT channel is matched automatically at the reference plane using amplitude calibration of the feedforward path. The developed system automatically calibrates the feedforward channel transmission characteristic to extract the measurement error and channel losses. Calibration is used to generate an output power characteristic as a function of power and frequency. This enables amplitude correction between the DUT and feedforward channels. The phase necessary to cancel the probe signal at the reference plane must still be obtained.

Cancellation methods using power minimization or gradient techniques are effective at eliminating phase error iteratively. However, the number of iterations to reach cancellation in excess of 30 dB can be large [4], [8], [13]. In the work described here, an approximation method is used to determine the phase shift necessary for cancellation given the amplitude of the combined feedforward and DUT signal. This results in greater speed and accuracy than can be obtained with iterative search methods. The approximation method is based on amplitude measurements which enables implementation using standard laboratory equipment such as a spectrum analyzer or a vector signal analyzer. Development of a predictive formula based on amplitude measurement can be obtained by first considering the cancellation of a single sinusoidal signal.

Consider a sinusoidal signal which is the combination of the stimulus signal and the feedforward signal [9]

$$\alpha \cos(\omega_1 t + \phi_1) + \alpha \cos(\omega_1 t + \phi_2) = \beta \cos(\omega_1 t + \phi_3) \quad (2)$$

where α is the amplitude of both the original and cancellation signal, ω_1 is the radian frequency of the signals, ϕ_1 is the phase of the original signal, ϕ_2 is the phase of the cancellation signal, ϕ_3 is the phase of the combined signal, and β is the amplitude of the combined signal. If the tone frequencies are the same and the signal propagation is in the same direction, the phase relationship between the tones is constant. The relationship between the tones can be evaluated at any time. Considering (2) at $t = 0$ and treating ϕ_3 as an arbitrary reference phase, (2) can be rewritten as a function of only the magnitude and phase differences as

$$\cos(\phi_1) + \cos(\phi_2) = \frac{\beta}{\alpha} \quad (3)$$

where ϕ_3 has been chosen to be zero. From trigonometric identities, it can be shown that

$$\cos(\phi_1) + \cos(\phi_2) = 2 \cos\left(\frac{\phi_1 + \phi_2}{2}\right) \cos\left(\frac{\phi_1 - \phi_2}{2}\right). \quad (4)$$

The phase of the combined signal is related to the phase of the cancellation and original signals by

$$\frac{(\phi_1 + \phi_2)}{2} = \phi_3 = 0. \quad (5)$$

Defining $\phi_1 - \phi_2$ as the phase difference ϕ , (3) and (4) become

$$\cos\left(\frac{\phi}{2}\right) = \frac{\beta}{2\alpha}. \quad (6)$$

Solving for the phase difference yields

$$\phi = n\pi \pm 2 \arccos\left(\frac{\beta}{2\alpha}\right), \quad n = 0, 1, \dots \quad (7)$$

The phase difference required for cancellation is π . Choosing $n = 0$ and rewriting in terms of the phase shift required for complete cancellation ϕ_s [9], we obtain

$$\phi_s = \pi \pm 2 \arccos\left(\frac{\beta}{2\alpha}\right). \quad (8)$$

There will be a phase prediction error, in general, which is the difference between the predicted phase shift and the ideal phase shift. This error tends to reduce as the signals approach 180° phase difference. The signal cancellation achieved by applying the predicted phase shift of (8) to the feedforward signal, when the post-DUT signal and feedforward signal amplitude is the same, is plotted versus signal phase difference in Fig. 1. The absolute phase error of the approximation formula is also shown against feedforward signal and probe-signal phase difference in Fig. 1. The accuracy of the approximation formula, assuming no amplitude error, is lowest when the two tones have a phase difference of 3° . At this point, 1.242° of phase error exists, limiting single iteration cancellation to 33 dB. Error reduces as the phase difference of the tones increases, lending itself to greatly increased accuracy upon a second application, in practice often exceeding 50 dB. Although the formula is derived to cancel only a single tone, it is extensible to other signals such as digital modulation and multisine, where the cancellation bandwidth can be derived from (1).

Equation (8) provides only the magnitude of the required phase shift. Thus, taking one of the solutions, say the positive phase shift, may not increase cancellation, and so the negative phase shift must then be used. With a vector signal analyzer used to measure both the phase and amplitude of the signal component being cancelled, it is possible to determine which phase-shift solution to use by determining the sign of β relative to α in (8). Implementation of (8) can be accomplished through the establishment of a reference cancellation plane. The reference plane is established by measuring the probe tone power and then measuring the power from the combination of the feedforward path and the DUT path signals at the bridge point. Their respective phases must also be measured if the sign of the phase

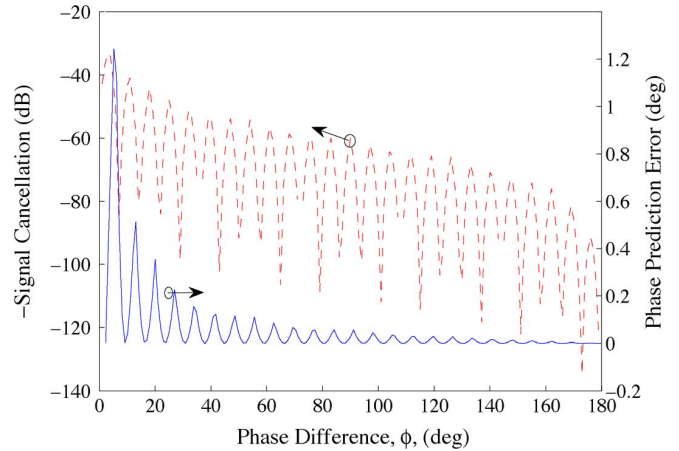


Fig. 1. Phase shift error of (8) versus phase difference between the stimulus signal and the feedforward signal from 0° to 180° . Also shown is the cancellation achievable with (8) if the amplitude of the stimulus and feedforward signal are equal.

shift is to be determined. Only two amplitude measurements are required to determine where the relative phase of the tones is on the unit circle before cancelling those tones. The following section details the construction of a feedforward system that implements (8).

III. FEEDFORWARD SYSTEM DESIGN

Feedforward cancellation is an application of the bridge method for measuring small variations in signals [15]. Typically, the feedforward and DUT paths of the bridge combine at a reference plane. Only the original signal will be fed forward and cancelled, enabling high-dynamic-range measurement of the unaffected DUT distortion components beyond the reference plane. A few practical issues arise that govern the implementation of the bridge technique including phase tracking of the cancellation signal and noise coherence. Both noise coherence and phase tracking are governed by the method used to generate the feedforward signal. The most prominent methods include separate sources, sampling and regenerating the signal with analog to digital and digital to analog converters, and coupling off of part of the original signal. Each of the feedforward signal generation methods and noise coherence effects are discussed in this section in the context of measurement system architecture, which is subsequently implemented.

Phase instability is an unavoidable issue when employing separate cancellation sources. Modern frequency-synthesizer architectures are frequency locked rather than being phase locked [16]. With frequency-locked sources, random phase variations of independent fractional synthesizers are only required to have on average a particular time-varying phase relationship. While this significantly reduces the level of spurious tones, this time-varying phase relationship causes the phase difference between two frequency-locked signals to wander. Using separate sources to provide the cancellation signals thus requires constant phase control to retain cancellation [9]. If continuous phase control is not employed, the result is typically a slow variation of a few decibels or complete loss of cancellation. Designs that sample or couple the original signal and

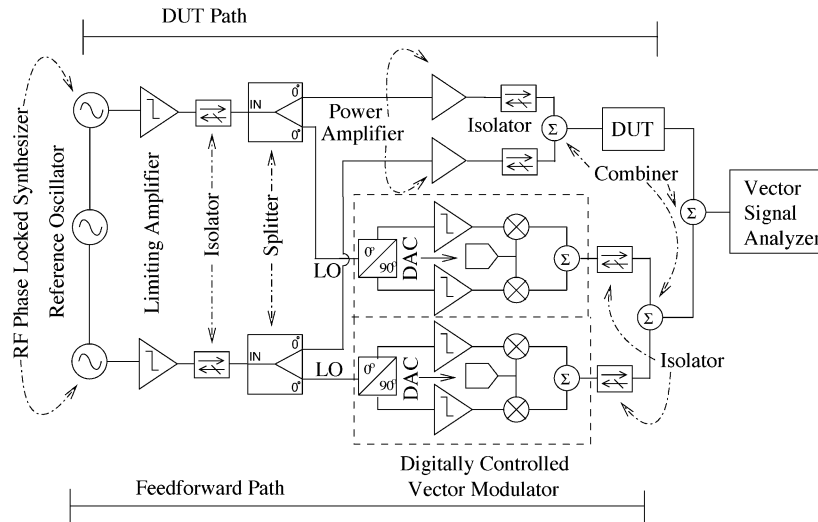


Fig. 2. High-dynamic-range PIM measurement system composed of highly linear amplifiers, RF sources, isolators, combiners, vector modulators, and a vector signal analyzer. Four separate DACs, represented by one DAC, are used to individually control the positive and negative in-phase and quadrature inputs of the vector modulators, shown with their internal schematics. The LO input of the vector modulators is identified.

use this to form the cancellation signal do not have this phase instability problem as the cancellation signal is inherently phase and frequency locked to the original signal.

Noise coherence only exists when coupling of the original signal is used. When separate sources are used, the noise in the cancellation signal is random with respect to the noise in the applied DUT signal. The noise from a sampled and regenerated signal is random with respect to the DUT channel unless the circuitry can sample both the noise and signal. The signals may be frequency and phase locked, but the noise will be independent and will sum. Noise summation detracts from the dynamic range of the system, and ultimately limits the capability of the measurement system. Feeding forward part of the original signal avoids this problem, as source noise is also fed forward and cancelled, leaving only the noise added by components such as the DUT, active devices, and passive components. Noise from these components is typically several orders of magnitude beneath the noise generated by the source.

A high-dynamic-range feedforward measurement system which couples off part of the original signal is shown in Fig. 2. Here the system is implemented for a two-tone signal with vector modulators used to control the phase and amplitude of the signals in the cancellation channels, replacing variable attenuators and delay lines. In the implementation described, the Hittite HMC497LP4 vector modulators have a bandwidth of 3.9 GHz, enabling nonlinear vector signal analysis from 100 MHz to 4 GHz. The vector modulators are controlled by dc voltages at the in-phase (I) and quadrature (Q) ports generated by digitally controlled 16-b resolution digital-to-analog converters (DACs). The DACs have a minimum output voltage increment of 0.305 mV and an error of 0.152 mV. The DAC-driven vector modulators provide up to 360° phase rotation and amplitude control between 20–40 dB for the feedforward signal, which is applied to the vector modulator local oscillator (LO) port. Isolators are used to limit the reverse traveling waves in the system which cause interchannel coupling if not suppressed. The two branches of the bridge, the cancellation channel and

the DUT channel, are finally summed at a reference plane before measurement by the vector signal analyzer.

The vector signal analyzer used in this system is the National Instruments NI-5660. It has a linearity of 80 dBc at the optimum input signal power of -33 dBm and a linearity of 73 dBc at an input signal power of -50 dBm. The sensitivity of the vector signal analyzer is -110 dBc at the optimal input signal power of -33 dBm and -92 dBc at a signal power level of -50 dBm. The sensitivity of the measurement system is increased over that of the vector signal analyzer sensitivity by the post-DUT cancellation of the stimulus signal and stimulus signal correlated noise. The cancellation achievable in this system is dependent on the accuracy of the phase shift and amplitude output of the vector modulators. In the system of Fig. 2, the amplitude output of the vector modulators is self-calibrated at a given feedforward signal input power automatically in software. The phase and amplitude accuracy of the feedforward channel is a function of I and Q gain, LO input power, vector modulator output power, and DAC accuracy. At optimum vector modulator output power, the phase accuracy of the feedforward channel is approximately 0.02° and the amplitude accuracy is approximately 0.006 dB. At a signal level 15 dB below the level of the optimum vector modulator output, the phase accuracy of the feedforward channel reduces to approximately 0.09° and the amplitude accuracy reduces to approximately 0.0265 dB. These accuracy levels, applied to (1), allow cancellation of approximately 62 dB. Thus, the phase and amplitude discretization error from the digitally controlled vector modulators does not limit the measurement system cancellation or dynamic range.

Reflected signals must be minimized at both the input and output ports as small reflected signals at the LO port of the vector modulator can be devastating to automated control. They can result in offsets in the amplitude of the output signal on the order of several decibels, high enough to cause loss of signal cancellation. The variation in output amplitude occurs due to the summation of the original and reflected waves within the vector modulator. If the reflected signal is much smaller than

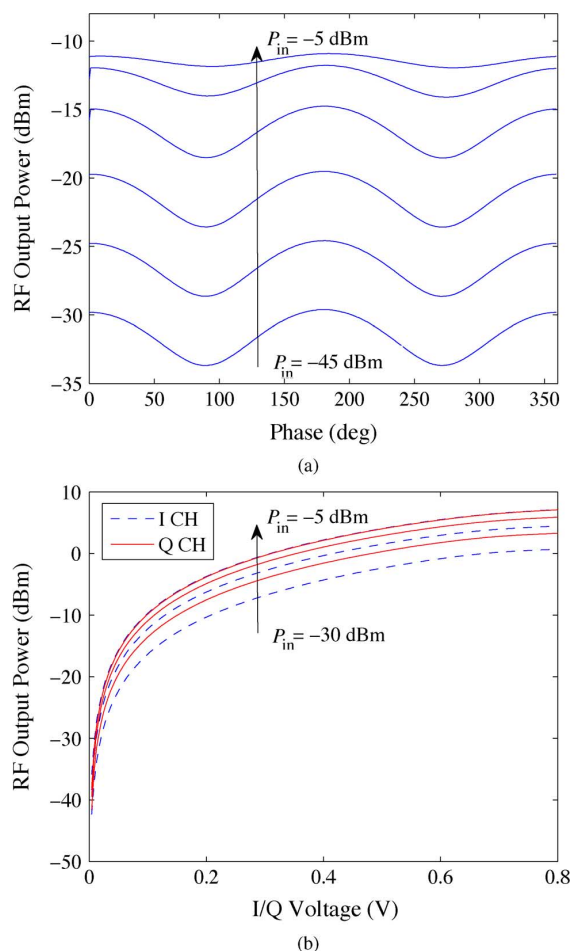


Fig. 3. Measured vector modulator response. (a) I/Q gains versus input LO drive power P_{in} below specification at -30 and -25 dBm, and within specification at -5 dBm. (b) Output power variation with output phase over input LO drive power, P_{in} , from -45 dBm to -20 dBm in 5-dBm increments.

the applied signal, and the gain is not balanced over input power between the I and Q channels, the smaller signal will experience different gains in the I and Q channels (in the linear mode). Fig. 3(a) compares the gains of the I and Q channels. It is shown that the gains are balanced only when the LO signal is sufficiently large to drive both of the I- and Q-channel mixers into their limiting mode of operation. As the LO level reduces below the limiting gain level, the I- and Q-channel gains become increasingly unbalanced. This leads to the much smaller reflected LO signal being amplified in linear mode and combined with the limited LO signal at a phase offset dependent on the reflected path characteristics and the linear mode I and Q gain differences. Eliminating this problem requires either suppression of the reflected signal or maintaining constant phase of the reflected wave over frequency. Software error correction can also be used to correct the behavior rather than eliminate it. In Fig. 3(b), a small interfering LO signal produces a linearly amplified output that oscillates with output phase due to gain imbalances. The cancellation occurring at the vector modulator output can be found from the combination of the linearly amplified reflected LO signal and the applied LO according to (1). For an applied local oscillator power of -5 dBm, the reflected

wave must be at least 40 dB below the applied signal to impact the output by less than 0.15 dB.

The feedforward architecture linearizes the receiver in the system by cancelling the large probe signal and its associated noise before reaching the receive circuitry. The distortion products generated by the DUT are left unaffected, increasing the dynamic range of the system if the stimulus signal generation circuitry is linear. Although the channels in the system of Fig. 2 are separated into a single tone per channel, interchannel coupling exists which limits the dynamic range achievable in the system. The effects of interchannel coupling and spurious frequency content on system dynamic range are discussed in Section IV.

IV. HIGH-DYNAMIC-RANGE DESIGN

Here, we discuss system design issues that must be addressed to achieve high-dynamic-range measurement of distortion signals in the presence of large signals. The achievable isolation between any two signal channels that are combined at a reference plane is limited and can result in weak intermodulation distortion (IMD) in each channel. Generation of IMD products can be caused by weak-reverse traveling waves interacting with large forward-traveling waves in active circuitry and isolation components. Spurious frequency content (spurs) from bias circuitry, sources, and radiative coupling between channels can also generate frequency content at the same frequencies as IMD products. Channel linearity is further dependent on passive component linearity. Each of these mechanisms reduces the dynamic range of the system and sets an ultimate limit on performance. Component linearity, spurious frequency content, and IMD due to reverse-wave interaction effects are discussed here.

A. Component Linearity

Selection of passive components with low distortion is vital for the high-power paths in the system. The choice of connector type employed throughout the high-power system paths generally specifies the passive IMD generated. According to [17], DIN- and N-type connectors plated with silver or trimetal exhibit superior PIM performance over smaller counterparts such as SMA-type connectors. The method of connector attachment must be chosen carefully to gain the benefits of connectors with larger contact area. Soldered connections are always preferable over clamped or crimped connections. Selection of hybrid combiners, directional couplers, attenuators, and cabling all follow the same connector guidelines and generate much less distortion than is measurable in the system developed here.

B. Spurious Frequency Content

Spurious frequency content (spurs) is often the limiting factor in system dynamic range. Any nonlinearity in a system path will alter the relationship between the spurs and the signal of interest, reducing or eliminating cancellation of the spurious content. The LO signal applied to the vector modulators undergoes mixing with any spurs coupled to the LO port through the process of hard limiting. Any signal coupling to the I and Q inputs of a vector modulator will also be upconverted by the mixers within the vector modulator. Spurious content altered by hard limiting or upconverted interference in the feedforward path will not cancel with the spurious content in the linear DUT

path due to the alteration of spur amplitude level and frequency spectrum. In this case, the spurs will sum and interact, reducing the dynamic range at frequencies in the vicinity of the spur. When using vector modulators to provide phase shift and attenuation, it is necessary to prelimit the signal before it is applied to the DUT and feedforward channels in order to achieve suppression of spurious signals. Prelimiting the signal ensures that the spurious frequency content is mirrored and maintains a defined relationship to the signal.¹

There are several sources of spurious frequency, including spurs induced in the bias circuitry and signal source spurs. Spurs from signal generators can be suppressed by prelimiting the signal or guaranteeing that both the DUT and vector modulator paths are linear. Ensuring that the paths are linear by driving the vector modulator far below its intended drive level would seem to be the logical choice. However, this would limit the output power effectively diminishing the achievable system dynamic range or would require power amplification. Prelimiting the signal before both the vector modulator and the DUT path predistorts the spurs and allows suppression of spurious content at the cancellation reference plane. In effect, this removes amplitude modulated distortion. Spurs from bias circuitry can be removed by the same process, but it is often not feasible to do so. If bias spurs are present in subsequent amplification stages or in the power supply of the vector modulator, a spectrum of harmonics resulting from ac power rectification will be mixed onto the original signal. Such spurs can only be removed by extracting the signal from farther down the signal path at often undesirable locations (such as after amplification). The only other alternatives for reducing these spurs are to use heavy EMI filtering or using dc power with clean bias networks.

C. Interchannel Coupling

The DUT path must have distortion lower than the dynamic range of the system, with the exception of the DUT itself. Key to this architecture is the use of individual linear amplifiers for each test signal and the effective backward-wave isolation provided by the isolators. Isolators are necessary to limit the output of the amplifier from nonlinear interaction with other stimuli through the finite isolation of the hybrid combiner. This isolation is important in the cancellation branch as well, where reflected-wave components can interact with the nonlinear junctions contained within the vector modulators. While isolators provide needed isolation, they also limit system bandwidth, and if not used carefully, produce distortion themselves. System bandwidth limitations can be overcome by using high-power switches designed for low PIM performance to switch between isolators in different bands. The distortion produced in the system due to reverse-wave interaction is largely due to interaction at the output of the amplifiers. This distortion is produced at an amplitude that is almost equivalent to that of the reverse wave less the directivity of the amplifier if the amplifier is being driven even remotely near the 1-dB compression point. The compressive nonlinearity in limiting amplifiers is now discussed as it affects both distortion generated by the reverse wave and interference induced by electromagnetic coupling.

¹See the Appendix for a full description of the mirroring effect in limited amplifiers.

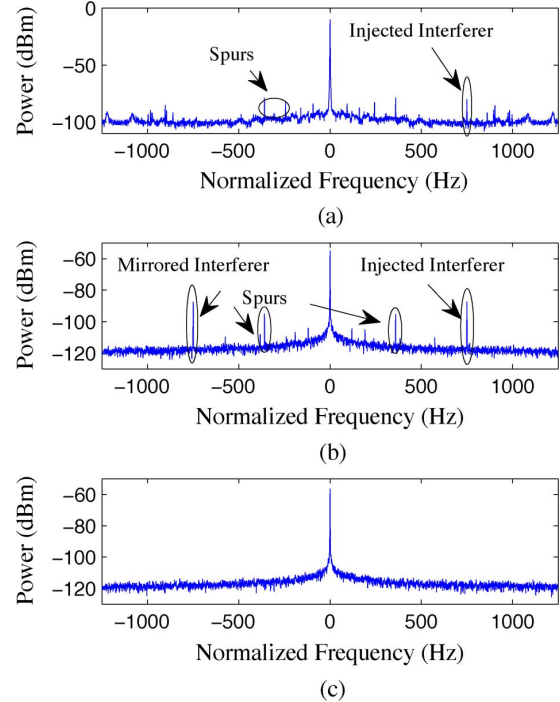


Fig. 4. Vector modulator response. (a) Spectrum showing an input signal composed of a single tone (the LO), spurious signals, and an injected interferer. (b) Spectrum showing mirrored interferer and spurious signals in cancelled output. (c) Spectrum with all spurious signals and the interferer removed when input signal is prelimited.

Due to the effect of limiting within any compressive nonlinearity, coupling from a secondary carrier will act as a spur which is translated directly to a third-order intermodulation frequency through mirroring (see the Appendix). The signal of Fig. 4(a) is the spectrum of a signal comprising a single tone (the LO), spurious content, and an injected interferer. In Fig. 4(b), the signal in Fig. 4(a) is cancelled without prelimiting being used. In Fig. 4(b), an injected interference tone is symmetrically mirrored around the LO frequency when the signal is not prelimited before cancellation. All spurious content is also left unaltered due to the mirrored components generated within the vector modulator. When the signal is prelimited before cancellation, the injected interferer is removed along with all spurious frequency content. The result is the clean cancelled spectrum shown in Fig. 4(c). The mirroring effect occurs due to the virtual elimination of the small spurious tones during the time period in which the LO is limited, equivalent to the multiplication of the spurious frequency content by a pulse train. Fig. 5 shows the response of an amplifier driven by a signal comprising a tone large enough to cause limiting and a small interfering tone. The original interferer is mirrored around the large signal according to²

$$\begin{aligned}
 P(f_p, t)[Gx_2(f_2, t)] &= \Im\{P\} * \Im\{x_2\} \\
 &= \int_{-\infty}^{\infty} P(\tau)x_2(\tau - f)d\tau
 \end{aligned} \tag{9}$$

²See the Appendix for a derivation of (9).

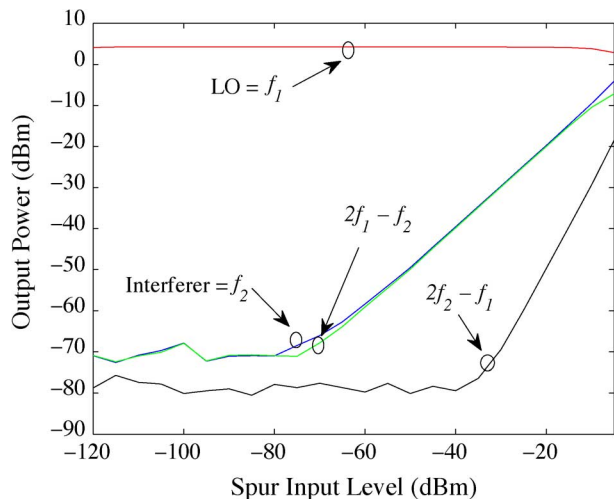


Fig. 5. Response of an amplifier driven into limiting by a signal composed of a large signal and a small interferer over interferer input power. The LO signal is at frequency f_1 while the interferer is at frequency f_2 . The interferer is mirrored around the carrier to the frequency $2f_1 - f_2$ at the same power level as the interferer and increases in a one-to-one relationship with the interferer. Frequency content generated at $2f_2 - f_1$ possesses a three-to-one relationship with the interferer and is generated at a much lower power level.

with the power of the mirrored signal increasing linearly with the interferer. Actual third-order distortion is not seen until the interferer signal becomes appreciable compared with the large signal. The effect is that dynamic range is reduced by about 40 dB.

Often interchannel coupling occurs which will be mirrored to intermodulation frequencies by the effect described above. Interchannel coupling can result from radiatively coupled components at the input to an amplifier because of the finite isolation of cables. This coupling can also result from a reverse signal traveling from one channel to another channel through the finite channel isolation in place to prevent reverse-wave interaction at the amplifier output. The coupling levels of these spurs are very different in the DUT and vector modulator paths and are thus extremely difficult to remove. Isolation must be provided to prevent the radiative coupling of other channels into the gain path of another channel as well as from reflected signals at the output of any active devices. The achievable isolation becomes the effective limiting factor on the dynamic range of the system. Accomplishing radiation isolation requires the complete shielding of every circuit in the cancellation path from any cable containing another channel. In the system of Fig. 2, the two channels are broken into two dual shielded rack-mountable chassis to ensure adequate isolation.

V. MEASUREMENT AND DISCUSSION

Two common situations often occur in distortion measurement: low-level IMD detection and high-level distortion products within the applied signal bandwidth. Cancellation can facilitate measurement in both of these situations, but alteration of the test setup is required. In the case of low-level IMD detection, such as is necessary in PIM testing, extreme dynamic range is accomplished by using multichannel cancellation and with prelimiting to enable spur suppression. Digitally modulated signals have both cochannel and adjacent channel interference. While

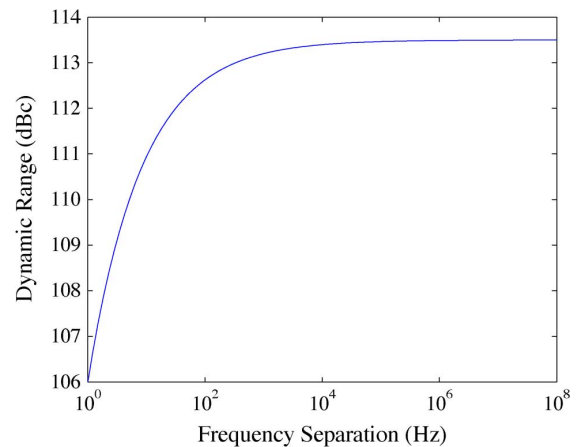


Fig. 6. Automated dynamic range obtained during two-tone testing over frequency separation of the tones.

adjacent channel interference has received much attention due to its ease of measurement, cochannel distortion is not directly observable from the spectral measurement of the output signal and is instead quantified by waveform signal quality metrics such as signal-to-noise and distortion ratio, error vector magnitude, and the correlation coefficient [18]. A single-channel linearly driven cancellation system can directly display the cochannel distortion by removing the original output signal. Dynamic range enhancement for PIM applications and digitally modulated signals are discussed in the following subsections.

A. Dynamic Range Enhancement for PIM Applications

In application of the system to PIM measurements, cancellation levels achieved for a two-tone signal were 35–40 dB over power and frequency for a single iteration of (8). This increased to approximately 50 dB upon a second iteration. This level of performance was achieved from 380 MHz to 1 GHz in the system of Fig. 2, limited by the power amplifiers and available isolators. Dynamic range of the system was increased to 113 dB at 5 W of output power for 100-Hz signal separations and above by suppressing radiative coupling and reflected signals while providing cancellation in excess of 40 dB. Even at tight signal separations of less than 10 Hz, at least 106 dB of dynamic range was obtained, as shown in Fig. 6. This limit was established by the uncorrelated phase noise of the reference oscillators. The finite resolution of amplitude measurements also impacted the dynamic range as it was the prominent source of cancellation error. Amplitude measurement error increased as the receiver became more saturated. Experimentally, the cancellation algorithm is more effective at lower power and can be reapplied to compensate for receiver saturation in high-power testing, where subsequent iterations return the receiver to linear operation.

B. Digitally Modulated Signals

The measurement system can also be used in distortion measurements with digitally modulated signals with results equal to or exceeding those in [6]–[8]. Prelimiting in both the DUT and feedforward paths by the limiting amplifiers in Fig. 2 allows correlated spurious frequency content to be suppressed along with the probe stimulus. With wideband signals such as wideband

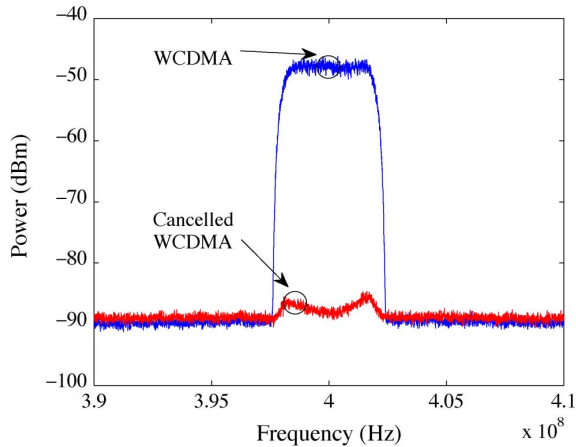


Fig. 7. WCDMA signal cancellation: Spectrum of the original WCDMA signal and the cancelled WCDMA signal at the output of the canceller with the DUT replaced by a through connection.

code-division multiple access (WCDMA), limiting operations such as those occurring in vector modulators result in a large degree of spectral regrowth. If the signal is driven within the LO input specification of the vector modulator, then the signal is distorted as if it were run through a limiting amplifier. Driving the LO port at a reduced power level results in linear mode operation in which the phase of the wideband signal can be altered without causing increases in the error vector magnitude of the applied signal. Typically, the noise associated with wideband signals significantly exceeds spurious frequency content from signal generators eliminating the need for spur suppression. The system of Fig. 2 was altered such that limiting amplifiers were removed, and only one stimulus channel and one feedforward channel were used for WCDMA testing.

The linear mode of operation, where the limiting amplifiers in Fig. 2 are removed, requires calibration as the gain paths are usually unbalanced. This calibration is carried out directly with WCDMA signals instead of discrete tones as in the high-dynamic-range PIM application case. Once this is accomplished, signal cancellation can be carried out normally, as long as the DUT path is linear except for the DUT itself. A WCDMA signal, shown in Figs. 7 and 8, was applied to the vector modulators in order to demonstrate the ability to operate with wideband signals when they are supplied to the vector modulator LO port instead of being upconverted through the I and Q inputs. In Fig. 7, cancellation in excess of 40 dB is demonstrated with no measurable spectral regrowth. The measured error vector magnitudes of the original WCDMA signal and the feedforward signal were 1.21% and 1.27%, respectively. The applied WCDMA signal, the output signal of a BGA2716 amplifier, and the remaining distortion components after cancellation in excess of 40 dB are shown in Fig. 8. The cancelled signal is offset by -5 dB to increase display intelligibility in Fig. 8.

Group delay differences of the feedforward and DUT paths limit the achievable cancellation bandwidth [8], [10]–[13]. Testing of devices with filters pronounces this effect greatly due to both a larger difference in constant group delay and frequency-dependent group delay response. This effect is illustrated in Fig. 9. The shape of the cancelled WCDMA signal

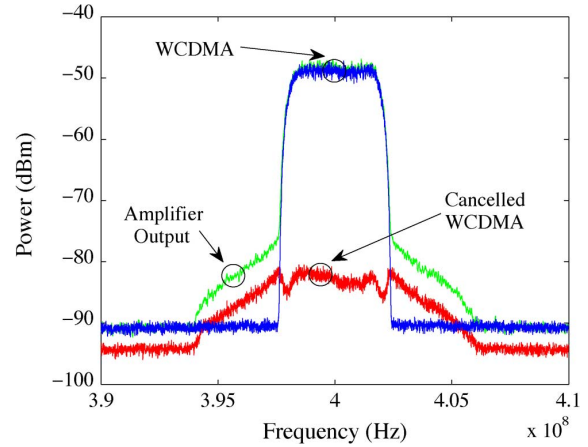


Fig. 8. WCDMA signal with an NXP BGA2716 wideband MMIC amplifier as the DUT. The original WCDMA signal is shown with the amplifier output exhibiting significant spectral regrowth. The cancelled WCDMA DUT signal, offset by -5 dB, is also shown revealing the uncorrelated in-band distortion masked by the original WCDMA signal.

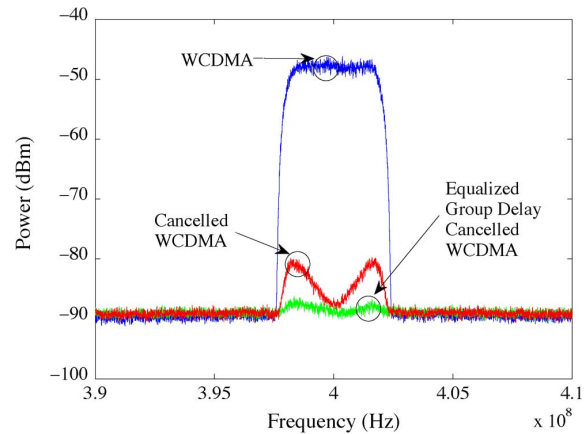


Fig. 9. WCDMA signal applied to a Mini-Circuits VLF-400 low-pass filter. Cancellation is shown for both equalized and unequalized group delay.

in Fig. 9 is the result of group delay mismatch when testing a Mini-Circuits VLF-400 low-pass filter as the DUT. The limited cancellation is due to the filter group delay response. Enhanced cancellation can be achieved by equalizing the group delay in the DUT and feedforward path. To examine this a second VLF-400 filter was inserted in the feedforward path after the vector modulator. Fig. 9 shows the impact of doing this by comparing the equalized group-delay-cancelled WCDMA spectrum with the spectrum of the “cancelled WCDMA” signal without group-delay equalization. Thus, approximate group-delay equalization effectively eliminates the bandwidth limitation that otherwise occurs.

VI. CONCLUSION

A broadband distortion measurement system with high dynamic range has been presented which employs an analytic model to predict the phase shift required to cancel a signal. This model uses only knowledge of the probing signal power and the combined probe and cancellation signal power. The model provides a rapid measurement capability limited only by the time required to reach steady state, approximately three

times the inverse of the tone separation. The system extends the dynamic range of IMD measurement for a two-tone signal by 40 dB. Used with a commercial vector signal analyzer, 113-dB dynamic range was achieved in a two-tone test system with tone separations of 100 Hz and above. This reduces monotonically to 106-dB dynamic range at 1 Hz tone separation. The operating bandwidth of the system is 380 MHz to 1 GHz limited principally by the bandwidth of available isolators. The system can also be used with digitally modulated signals where uncorrelated distortion is of interest, as was demonstrated for a WCDMA signal, with cancellation in excess of 40 dB at an error vector magnitude of 1.27%. Pre-distortion of both group delay and mirroring effects in a feedforward system have been demonstrated as an effective means of increasing dynamic range through cancellation of delay mismatch and spurious frequency content.

APPENDIX

This Appendix addresses the spectrum at the output of an amplifier resulting from the combination of a large signal with a small signal. The large signal has sufficient amplitude to drive the amplifier into compression. It is shown that the output spectrum contains frequency components corresponding to the large and small input tones as well as the image of the small signal with respect to the large signal. The signal and image sidebands are also at the harmonics of the large signal. Consider the signal $x_1(t) + x_2(t)$, defined by

$$x_1(t) = A_1 \sin(2\pi f_1 t + \phi_1) \quad (10)$$

$$x_2(t) = A_2 \sin(2\pi f_2 t + \phi_2) \quad (11)$$

applied to the input of an amplifier. The amplitude, frequency, and phase of the respective signals are given by A_1 , A_2 , f_1 , f_2 , ϕ_1 , and ϕ_2 , respectively. If the amplitude A_1 is much larger than the amplitude of A_2 and larger than the input saturation amplitude of the amplifier A_s , limiting will occur on the amplified combined signal $x_1(t) + x_2(t)$. The smaller signal $x_2(t)$ experiences gain only when the larger signal is less than A_s ; its contribution to the output is effectively reduced to zero when $x_1(t)$ is above A_s . The sudden reduction of signal amplitude to zero is equivalent to the multiplication of a pulse train $P(f_p, t)$ with $x_2(t)$, where $P(f_p, t)$ is defined in the period of $x_1(t)$ as

$$\begin{aligned} P(f_p, t) = & u\left(t - \frac{1}{2\pi f_1} \arcsin(A_s/A_1)\right) - \dots \\ & u\left(t - \frac{1}{2f_1} + \frac{1}{2\pi f_1} \arcsin(A_s/A_1)\right) + \dots \\ & u\left(t - \frac{1}{2f_1} - \frac{1}{2\pi f_1} \arcsin(A_s/A_1)\right) - \dots \\ & u\left(t - \frac{1}{f_1} + \frac{1}{2\pi f_1} \arcsin(A_s/A_1)\right) + A_0. \quad (12) \end{aligned}$$

A_0 represents an arbitrary offset dependent on the amplifier and f_p is defined as the sampling frequency of the pulse train relative to $x_2(t)$.

Both positive and negative limiting result in the small signal $x_2(t)$ being reduced to zero amplitude. The frequency of the

pulse train f_p is then twice the rate of the frequency of the large limiting signal $x_1(t)$. The mixing spectrum associated with the multiplication of signal $P(f_p, t)$ and signal $x_2(t)$ can be obtained by convolving the Fourier transform of the respective signals

$$\begin{aligned} P(f_p, t)[Gx_2(t)] &= \mathfrak{F}\{P\} * \mathfrak{F}\{x_2\} \\ &= \int_{-\infty}^{\infty} P(\tau)x_2(\tau - f)d\tau \quad (13) \end{aligned}$$

where G is the gain the small signal experiences, defined by

$$G = \frac{g \int_0^{1/\Delta f} |P_i(\tau)x_2(\tau)|d\tau}{\int_0^{1/\Delta f} |x_2(\tau)|d\tau}. \quad (14)$$

In (14), g is the linear small-signal gain of the amplifier and P_i is defined as

$$P_i(f_p, t) = 1 - P(f_p, t). \quad (15)$$

The spectrum will consist of a mirrored image of the signal $x_2(t)$ around the large signal $x_1(t)$ and its harmonics at a frequency separation Δf of $|f_1 - f_2|$. The extent of mirroring around the harmonics will depend upon the symmetry and offset of the limiting operation.

REFERENCES

- [1] J. R. Wilkerson, K. G. Gard, and M. B. Steer, "Electro-thermal passive intermodulation distortion in microwave attenuators," in *Proc. 36th Eur. Microw. Conf.*, Sep. 2006, pp. 157–160.
- [2] J. R. Wilkerson, K. G. Gard, A. G. Schuchinsky, and M. B. Steer, "Electro-thermal theory of intermodulation distortion in lossy microwave components," *IEEE Trans. Microw. Theory Tech.*, vol. 56, no. 12, pp. 2717–2725, Dec. 2008.
- [3] E. Rubiola and V. Giordano, "Advanced interferometric phase and amplitude noise measurements," *Rev. Sci. Instrum.*, vol. 73, no. 6, pp. 2445–2457, Jun. 2002.
- [4] S. P. Stapleton, "Adaptive feedforward linearization for rf power amplifiers," in *Proc. 55th Autom. RF Tech. Group Conf.*, Jun. 2000, pp. 1–7.
- [5] B. Deats and R. Hartman, "Measuring the passive intermodulation performance of rf cable assemblies," Summitek Instruments, Parker, CO, pp. 1–8. [Online]. Available: <http://www.summitekinstruments.com/passive/docs/cablepim.pdf>.
- [6] V. Aparin and L. E. Larson, "Analysis and reduction of cross-modulation distortion in CDMA receivers," *IEEE Trans. Microw. Theory Tech.*, vol. 51, no. 5, pp. 1591–1602, May 2003.
- [7] J. C. Pedro and N. B. Carvalho, "Evaluating co-channel distortion ratio in microwave power amplifiers," *IEEE Trans. Microw. Theory Tech.*, vol. 49, no. 10, pp. 1777–1784, Oct. 2001.
- [8] O. Andersen, D. Wisell, and N. Keskitalo, "Measurement of aclr with high dynamic range," in *IEEE MTT-S Int. Microw. Symp. Dig.*, Jun. 2008, pp. 273–277.
- [9] J. R. Wilkerson, K. G. Gard, and M. B. Steer, "Wideband high dynamic range distortion measurement," in *Proc. IEEE Radio and Wireless Symp.*, Jan. 2008, pp. 415–418.
- [10] K. J. Parsons and P. B. Kenington, "Effect of delay mismatch on a feedforward amplifier," *Proc. Inst. Elect. Eng.—Circuits, Devices Syst.*, vol. 141, pp. 140–144, Apr. 1994.
- [11] S. Kang, Y. Jung, and I. Lee, "Novel analysis of the cancellation performance of a feedforward amplifier," in *Proc. IEEE Global Commun. Conf.*, Nov. 1997, pp. 72–76.
- [12] R. J. Wilkinson and P. B. Kenington, "Specification of error amplifiers for use in feedforward transmitters," *Proc. Inst. Elect. Eng.—Circuits, Devices Syst.*, vol. 139, no. 4, pp. 477–480, Aug. 1992.

- [13] A. Roussel, C. Nicholls, and J. Wright, "Frequency agile RF feedforward noise cancellation system," in *Proc. IEEE Radio Wireless Symp.*, Jan. 2008, pp. 109–112.
- [14] N. Potheary, *Feedforward Linear Power Amplifiers*. London, U.K.: Artech House, 1999.
- [15] N. Krikorian, "Bridge method for measuring amplitude intermodulation distortion," *RF Design*, pp. 30–34, Mar. 1995.
- [16] A. Walker, M. Steer, and K. Gard, "Simple, broadband relative phase measurement of intermodulation products," in *Proc. 65th Autom. RF Tech. Group Conf.*, Jun. 2005, pp. 123–127.
- [17] J. Henrie, A. Christianson, and W. Chappell, "Prediction of passive intermodulation from coaxial connectors in microwave networks," *IEEE Trans. Microw. Theory Tech.*, vol. 56, no. 1, pp. 209–216, Jan. 2008.
- [18] K. M. Gharaibeh, K. G. Gard, and M. B. Steer, "Estimation of cochannel nonlinear distortion and SNDR in wireless systems," *IET Microw., Antennas, Propag.*, vol. 1, no. 5, pp. 1078–1085, Oct. 2007.



Jonathan R. Wilkerson (S'08) was born in Greenville, NC. He received the B.S. degree in electrical engineering and computer engineering and the M.S. degree in electrical engineering from North Carolina State University, Raleigh, in 2005 and 2006, respectively, and is currently working toward the Ph.D. degree at North Carolina State University.

He is currently a Graduate Research Assistant with the ERL Laboratory, Electrical and Computer Engineering Department, North Carolina State University.



Kevin G. Gard (S'92–M'95) received the B.S. and M.S. degrees from North Carolina State University, Raleigh, in 1994 and 1995, respectively, and the Ph.D. degree from the University of California at San Diego, La Jolla, in 2003, all in electrical engineering.

He is currently the William J. Pratt Assistant Professor with the Electrical and Computer Engineering Department, North Carolina State University. From 1996 to 2003, he was with Qualcomm Inc., San Diego, CA, where he was a Staff Engineer and Manager responsible for the design and development of radio frequency integrated circuits (RFICs) for code-division multiple-access (CDMA) wireless products. He has designed SiGe BiCMOS, Si BiCMOS, and GaAs metal–semiconductor field-effect transistor (MESFET) integrated circuits for cellular and personal communication systems (PCSs) CDMA, WCDMA, and AMPS transmitter applications. His research interests are in the areas of IC design for wireless applications and analysis of nonlinear microwave circuits with digitally modulated signals. He has authored or coauthored over 60 papers related to RF/analog IC design and analysis of nonlinear circuits.

Dr. Gard is a member of the IEEE Microwave Theory and Techniques Society (IEEE MTT-S) and the IEEE Solid-State Circuits Society, Eta Kappa Nu, and Tau Beta Pi. In 2007, he was secretary of the IEEE MTT-S AdCom.



Michael B. Steer (F'99) received the B.E. and Ph.D. degrees from the University of Queensland, Brisbane, Australia, in 1976 and 1983, respectively, both in electrical engineering.

He is the Lampe Professor of Electrical and Computer Engineering with North Carolina State University, Raleigh. In 1999 and 2000, he was a Professor and Director of the Institute of Microwaves and Photonics, University of Leeds, Leeds, U.K., where he held the Chair in Microwave and Millimeter-wave Electronics. He has authored or coauthored more than 400 publications on topics related to nonlinear RF effects, circuit-field simulation, RF behavioral modeling, microwave and millimeter-wave systems, high-speed digital design, and RF/microwave design methodology. He is an expert on circuit-field interactions. He has authored three books, *Microwave and RF Design: A Systems Approach* (SciTech, 2008), *Foundations of Interconnect and Microstrip Design* (with T.C. Edwards) (Wiley, 2000), and *Multifunctional Adaptive Microwave Circuits and Systems* (with W. D. Palmer) (SciTech, 2009).

Prof. Steer was secretary of the IEEE Microwave Theory and Techniques Society (IEEE MTT-S) in 1997, and, from 1997 to 2000 and 2003 to 2006 was a member of the IEEE MTT-S Administrative Committee. He was Editor-in-Chief of the IEEE TRANSACTIONS ON MICROWAVE THEORY AND TECHNIQUES from 2003 to 2006. He is a 1987 Presidential Young Investigator and was the recipient of the Bronze Medallion by U.S. Army Research for "Outstanding Scientific Accomplishment" in 1994 and 1996. He was the recipient of the Alcoa Foundation Distinguished Research Award from North Carolina State University in 2003.